

## Supplementary Material

### **Dynamics of standing dead wood and severe fire in north Australian savannas: implications for carbon management**

*Peter J. Whitehead<sup>A,B</sup>, Brett P. Murphy<sup>C</sup>, Jay Evans<sup>A</sup>, Dominique Lynch<sup>D</sup>, Cameron P. Yates<sup>A,\*</sup>, Andrew Edwards<sup>A</sup>, Harry Mcdermott<sup>A</sup> and Jeremy Russell-Smith<sup>A,B</sup>*

<sup>A</sup>Charles Darwin University, Darwin Centre for Bushfires Research, Darwin, NT 0909, Australia

<sup>B</sup>North Australian Indigenous Land and Sea Management Alliance, Brinkin, NT 0810, Australia

<sup>C</sup>Charles Darwin University, Faculty of Science and Technology, Darwin, NT 0909, Australia

<sup>D</sup>Northern Territory Government, Department of Environment Parks and Water Security, PO Box 496, Palmerston, NT 0831, Australia

\*Correspondence to: Email: [cameron.yates@cdu.edu.au](mailto:cameron.yates@cdu.edu.au)

## SUPPLEMENTARY MATERIAL

Peter J. Whitehead<sup>a,b</sup>, Brett P. Murphy<sup>c</sup>, Jay Evans<sup>a</sup>, Dominique Lynch<sup>a</sup>, Cameron P. Yates<sup>a</sup>, Andrew Edwards<sup>a</sup>, Harry Mcdermott<sup>a</sup> and Jeremy Russell-Smith<sup>a,b</sup> (submitted). Dynamics of standing dead wood and severe fire in north Australian savannas: implications for carbon management.

*International Journal of Wildland Fire.*

### Table of Contents

Section 1: Details of variables included in statistical analyses. ....	2
Section 2: Model selection tables.....	5
Section 3: Statistical models - additional visualisation graphics .....	13
Section 4: Simulations - additional graphics.....	19
Section 5: Simulations- additional graphics on sequestration performance .....	31
Section 6: Species differences in stag dynamics .....	36
Section 7: Fire timing and projected sequestration performance .....	37

## Section 1: Details of variables included in statistical analyses.

Table S1: Variables recorded in the present study and/or extracted from other sources and used in statistical analyses.

Name	Description	Units	Source(s) where relevant
<b>Responses</b>			
surv	status of each tree stem as alive or dead	binary: dead=0, alive=1	
loss	status of each stag: gone (consumed) or fallen (from below breast height)	binary: lost=0, standing above breast height=1	
dbh	stem diameter at breast height	in cm at each visit, both live stems and stags	
rec	new stems >5 cm dbh	added as new observation, including secondary stems	
<b>Fire</b>			
fmi	mild fires	frequency (count)	fire severity categorisations from Russell-Smith and Edwards (2006) <sup>1</sup>
fmo	moderate fires	frequency (count)	
fse	severe fires	frequency (count)	
afmi	mild fires	relative frequency (annualised)	
afmo	moderate fires	relative frequency (annualised)	
afse	severe fires	relative frequency (annualised)	
tsfmi	time since mild fire in plot	years prior to visit at which fire recorded	
tsfmo	time since moderate fire in plot	years prior to visit at which fire recorded	
tsfse	time since severe fire in plot	years prior to visit at which fire recorded	
<b>Rainfall</b>			
mar	mean annual rainfall at each plot	in mm annual rainfall (rain-year: July to June). Plot average over the period 1972 to 2018	intersection with monthly rainfall grids (0.05 by 0.05 degrees). Jones et al. 2009 <sup>2</sup> .

<b>Name</b>	<b>Description</b>	<b>Units</b>	<b>Source(s) where relevant</b>
ri	index of rainfall at each plot between visits	ratio of within interval rainfall to long-term averages for the same plot over the same period	
ari	annualised rainfall index at each plot between visits	ri annualised by length of visit interval in years	
ry0	index for single rainy year ending immediately prior to visit		
ryi	index based on rainfall in all full rain-years ending within the visit interval	summed index divided by number of included rain-years	
<b>Plot features</b>			
plotid	unique identifier of each plot	comprising 3 transects	
stemid	unique identifier of all monitored stems within plots		
sp	species of each stem within plots		
vft	vegetation-fuel type class (VFT)	5 classes: OWM (open woodland, mixed u/s); SHH (shrubby heath); WHu (woodland with hummock grassland); WMi (woodland with mixed u/s); WTu (woodland with tussock u/s).	Lynch et al. 2015 <sup>23</sup> ; field observations, this study
top	landscape topography	6 broad topographic descriptors: plains or gently undulating; broad plateaus; dissected plateaus; stony hills; dissected lowlands; and floodplains and margins). A single dissected lowland site with one member was grouped with plains/gently undulating.	NRIC (1991) <sup>4</sup> : collapsed 43 units based on digitised mapping of landscape structure and soil types collapsed

<b>Name</b>	<b>Description</b>	<b>Units</b>	<b>Source(s) where relevant</b>
slo	slope	slope in degrees (as tangent in analysis)	NASA 2015 <sup>5</sup> (digital elevation model)
asp	aspect	aspect (orientation of slope) in 4 categories (N,E,S,W)	NASA 2015 (DEM)
ele	elevation	m above sea level	NASA 2015 (DEM)
si	soil index	4 categories: deep, shallow or skeletal sands, and clay	this study
ba	basal area (m <sup>2</sup> ha <sup>-1</sup> )	tree basal area at beginning of plot observations	this study

<sup>1</sup>Russell-Smith J, Edwards AC (2006) Seasonality and fire severity in savanna landscapes of monsoonal northern Australia. *International Journal of Wildland Fire* , **15**, 541-550.

<sup>2</sup>Jones, D. A., W. Wang, and R. Fawcett. 2009. High-quality spatial climate data-sets for Australia. *Australian Meteorological and Oceanographic Journal* **58**, 233.

<sup>3</sup>Lynch D, Cuff N, Russell-Smith, J. (2015) Vegetation fuel type classification for lower rainfall savanna burning abatement projects. Pp 73-96 In: Murphy BP, Edwards AC, Meyer CP, Russell-Smith J. (Eds.) Carbon accounting and savanna fire management (CSIRO Publishing, Melbourne)

<sup>4</sup>National Resource Information Centre. 1991. Digital Atlas of Australian Soils. Bureau of Resource Sciences (Canberra)

<sup>5</sup>NASA. 2015. The Shuttle Radar Topography Mission (SRTM) Collection User Guide. NASA (Sioux Falls, South Dakota)

## Section 2: Model selection tables

**Table S2: Summary of plot-level fire exposure and rainfalls by vegetation-fuel types (VFT). All-plot means are weighted by number of plots in VFT classes.**

VFT	Fire frequency (fires y <sup>-1</sup> )						Rainfall (rain-year mm y <sup>-1</sup> )		N
	Mild		Moderate		Severe		mean	range	
	mean	range	mean	range	mean	range			
OWM	0.164	0-0.625	0.151	0-0.500	0.062	0-0.286	824.1	147.8-2106.3	66
SHH	0.000	0-0.000	0.000	0-0.000	0.125	0-0.125	614.1	291.5-1311.3	1
WHu	0.162	0-0.333	0.206	0-0.556	0.063	0-0.143	968.0	345.6-2172.2	7
WMi	0.253	0-0.778	0.167	0-0.556	0.070	0-0.333	991.2	305.2-1901.0	22
WTu	0.266	0-0.700	0.148	0-0.556	0.043	0-0.200	899.6	396.8-2098.8	14
<b>All VFT</b>	<b>0.193</b>	<b>0-0.778</b>	<b>0.156</b>	<b>0-0.556</b>	<b>0.062</b>	<b>0-0.333</b>	<b>874.4</b>	<b>147.8-2172.2</b>	<b>110</b>

**Table S3: Statistical models relating stem survival between observations to stem DBH (cm) and fire and rainfall quanta within observation intervals, ordered on AICc. Predictors (fixed effects) additional to DBH are: number of fires during intervals between observations (fmi=mild, fmo=moderate, fse=severe); annualised fire frequency (asmi, afmo, afse); and rainfall variation index (ri=ratio of actual rainfall to long term mean for the observation interval at the relevant site). Random effects are tree species, plotID, soil index, mean long term annual rainfall, plot basal area, and vegetation-fuel type.**

Inter- cept	s-dbh	afse	afmo	afmi	fse	fmo	fmi	ri	df	logLik	AICc	ΔAICc
3.256	+	-0.962	-0.346	0.161				0.311	13	-4111.5	8203.8	0
3.276	+	-0.992	-0.376					0.329	12	-4112.4	8203.9	0.1
3.214	+	-0.926						0.328	11	-4095.7	8213.4	9.6
3.224	+				-0.737	-0.269	0.001	0.367	13	-4095.2	8216.3	12.5
3.182	+				-0.701			0.350	11	-4101.2	8224.3	20.5
3.593	+	-0.921							10	-4105.7	8231.3	27.5
3.582	+				-0.664				10	-4112.5	8245.0	41.2
3.212	+					-0.232		0.336	11	-4114.4	8250.8	47.0
3.151	+			0.302				0.287	11	-4115.0	8252.1	48.3
3.218	+		-0.273					0.321	11	-4115.7	8253.1	49.3
3.176	+							0.321	10	-4118.8	8257.7	53.9
3.173	+						0.065	0.301	11	-4118.4	8258.7	54.9
3.466	+			0.377					10	-4122.4	8264.8	61.0
3.593	+					-0.207			10	-4124.9	8269.9	66.1
3.590	+		-0.276						10	-4125.3	8270.6	66.8
3.490	+						0.139		10	-4126.1	8272.1	68.3
3.547	+								9	-4128.5	8275.0	71.7

**Table S4: Summary of model parameters for best within-observation-interval model for stem survival and fire and rainfall predictors ranked on AICc. Intercorrelations causes coefficients for different fire intensities to be labile when together in different combinations and hence the coefficients are individually unreliable.**

<b>A. parametric coefficients</b>	<b>Estimate</b>	<b>Std. Error</b>	<b>t-value</b>	<b>p-value</b>
(Intercept)	3.2561	0.2105	15.4690	<0.0001
afse	-0.9625	0.1295	-7.4309	<0.0001
afmo	-0.3460	0.1098	-3.1506	0.0016
afmi	0.1612	0.1136	1.4190	0.1559
ri	0.3112	0.0754	4.1250	<0.0001
<b>B. smooth terms</b>	<b>edf</b>	<b>Ref.df</b>	<b>F-value</b>	<b>p-value</b>
s(dbh)	5.6014	5.6014	209.2148	<0.0001



**Table S5: Candidate statistical models, ordered on AICc, relating stem survival between observations to stem DBH (cm) and fire and rainfall events falling entirely within and/or extended to include events preceding those intervals. Predictors (fixed effects) additional to DBH are: time since last mild, moderate or severe fire at the observation date, as ordered factors (tsfse, tsfmo, tsfmi); the rainfall variation index within the observation interval (ri) and extended to include all full rain-years ending in the years of consecutive visits (ryi); and the rainfall index for the most recent full rain-year ending in the year of interval end (ry0). Random effects are tree species, plotID, soil index, mean long term annual rainfall, plot basal area, and vegetation-fuel type (VFT). The highest ranked model based exclusively on within-interval fire (annualised) and rainfall variables (ri) (Table S4) is included (bold and italicised) for comparison with models using beyond-interval explanatory variables.**

Intercept	within interval variable							beyond interval variable				df	logLik	AICc	ΔAICc
	s-dbh	afse	afmo	afmi	ri	ari	ry0	ryi	tsfse	tsfmo	tsfmi				
2.663	+							0.933	+			13	-4037.0	8099.9	0
3.429	+				0.238				+			13	-4051.3	8128.5	28.6
3.469	+					0.284			+			13	-4052.0	8130.0	30.1
3.427	+						0.27		+			13	-4053.7	8133.3	33.4
3.712	+								+			12	-4056.1	8136.2	36.3
<b>3.256</b>	+	<b>-0.965</b>	<b>-0.346</b>	<b>0.161</b>	<b>0.311</b>							<b>12</b>	<b>-4111.5</b>	<b>8203.8</b>	<b>103.9</b>
3.384	+				0.276					+		13	-4111.3	8248.4	148.5
3.104	+				0.305						+	13	-4113.7	8253.4	153.5
3.176	+				0.321							10	-4118.8	8257.7	157.8
3.721	+									+		12	-4117.8	8259.6	159.7
3.459	+										+	12	-4122.2	8268.3	168.4

**Table S6: Summary of candidate statistical models for annual probability of stag persistence (1- stag loss) ranked by AICc. All candidates include the same suite of random effects stemID, plotID, species, soi, mar, ba and VFT. Abbreviations for fixed effects are given in previous model summaries (for mortality). Colons separating vector names indicate interactions. Although not shown here, models including interactions between fire and stag origin were invariably poorer fits than other candidates. We have included moderate/mild fire in models compared here only to illustrate the poorer fits and comparatively weak influence of fires of lower than severe intensities. We note that models including mild fire vectors, in addition to generating weaker fits, also had implausible positive (albeit non-significant,  $P>0.05$ ) coefficients, probably a product of inter-correlation with other (fire) covariates.**

Int s.	or	yas	or:	fmo	afmo	fse	afse	tsfmo	tsfse	ri	ri:	ari	ari:	ry0	ry0:	ryi	ryi:	df	logLik	AICc	$\Delta$	wt
	dbh		yas								yas		yas		yas		yas					
0.5	+	+	0.21	+			-0.79							1.43	-0.28			16	-1469.2	2970.5	0.0	0.9
1.9	+	+	-0.07	+			-0.80			0.92	-0.16							16	-1472.3	2976.8	6.3	0.0
0.3	+	+	0.25	+										1.54	-0.31			15	-1475.1	2980.3	9.8	0.0
1.2	+	+	0.04	+			-0.87				0.73	-0.12						16	-1474.4	2980.9	10.4	0.0
0.7	+	+	0.12	+			-0.85								1.17	-0.18		16	-1475.0	2982.2	11.7	0.0
1.9	+	+	-0.07	+			-0.87			0.29								15	-1476.3	2982.6	12.1	0.0
1.5	+	+	-0.06	+			-0.89							0.42				15	-1476.3	2982.7	12.2	0.0
1.3	+	+	-0.07	+			-0.87								0.57			15	-1476.5	2983.2	12.7	0.0
1.7	+	+	-0.06	+			-0.92				0.24							15	-1477.7	2985.5	15.0	0.0
1.9	+	+	-0.08	+			-0.89											14	-1478.9	2985.9	15.4	0.0
1.8	+	+	-0.06	+						1.03	-0.18							15	-1478.3	2986.7	16.1	0.0
1.9	+	+	-0.07	+			-0.64											14	-1480.7	2989.6	19.1	0.0
1.2	+	+	0.06	+							0.75	-0.14						15	-1481.4	2993.0	22.5	0.0
0.5	+	+	0.15	+												1.29	-0.21	15	-1481.8	2993.8	23.2	0.0

Int s.	or	yas	or:	fmo	afmo	fse	afse	tsfmo	tsfse	ri	ri:	ari	ari:	ry0	ry0:	ryi	ryi:	df	logLik	AICc	Δ	wt
dbh			yas								yas		yas		yas		yas					
1.8	+	+	-0.06	+						0.31								14	-1483.5	2995.1	24.5	0.
																						0
1.2	+	+	-0.06	+												0.60		14	-1483.7	2995.6	25.1	0.
																						0
1.4	+	+	-0.06	+										0.42				14	-1483.9	2995.8	25.3	0.
																						0
1.9	+	+	-0.07	+					+									16	-1482.0	2996.0	25.5	0.
																						0
1.8	+	+	-0.07	+	0.19													14	-1485.2	2998.5	28.0	0.
																						0
1.9	+	+	-0.07	+														13	-1486.5	2999.1	28.6	0.
																						0
1.6	+	+	-0.05	+							0.20							14	-1485.7	2999.5	29.0	0.
																						0
1.9	+	+	-0.07	+														14	-1486.5	3001.1	30.6	0.
																						0
1.8	+	+	-0.05	+					+									16	-1485.1	3002.4	31.9	0.
																						0
2.2	+	+	-0.18															12	-1489.2	3002.5	32.0	0.
																						0
1.7	+	+																11	-1518.0	3058.1	87.6	0.
																						0
1.8	+																	10	-1520.0	3060.1	89.6	0.
																						0

**Table S7: Candidate statistical models, ranked on AICc, for annualised growth increment between visits (agriv in mm y<sup>-1</sup>) and rainfall and fire frequency and timing. Prefix “p” and superscript “2” used with other vector names are quadratic orthogonal polynomials (using R function poly()). Abbreviations are otherwise as used elsewhere. Random effects were also the same as used in other models for mortality and stag loss.**

Int	dbh	fate	fse	fmo	fmi	afse	afmo	afmi	ri	pri <sup>2</sup>	ry02	pry0 <sup>2</sup>	ryi	pryi <sup>2</sup>	tsfse	tsfmo	tsfmi	df	logLik	AICc	ΔAIC
0.99	0.010	+								+					+			14	-72542.1	145112	0
1.00	0.010	+									+	+			+			14	-72563.8	145156	44
0.96	0.010	+								+								11	-72597.9	145218	106
-0.33	0.009	+						1.178										13	-72619.1	145264	152
0.96	0.010	+										+						11	-72629.6	145281	169
-0.58	0.010	+									1.483							13	-72647.7	145321	209
-0.36	0.009	+						1.144								+		13	-72655.2	145336	234
-0.39	0.010	+					0.204	1.179										11	-72669.0	145360	248
-0.38	0.010	+			-0.114			1.212										11	-72669.1	145360	248
-0.38	0.010	+		0.154				1.178										11	-72669.9	145362	250
-0.37	0.010	+						1.183										10	-72671.2	145362	250
-0.27	0.010	+						1.149								+		13	-72669.6	145365	253
-0.37	0.010	+				-0.119		1.185										11	-72671.9	145366	254
-0.37	0.010	+	-0.033					1.184										11	-72672.3	145367	255
-0.37	0.010	+						-0.013	1.185									11	-72673.1	145368	256
-0.66	0.009	+								1.468						+		13	-72681.6	145389	277
-0.62	0.010	+		0.166						1.470								11	-72703.1	145428	300
-0.62	0.010	+					0.176			1.470								11	-72703.8	145430	318
-0.61	0.010	+								1.477								10	-72705.0	145430	318
-0.61	0.010	+	0.132							1.476								11	-72705.6	145433	321
-0.61	0.010	+				-0.069				1.478								11	-72705.8	145434	322
-0.61	0.010	+						0.044		1.472								11	-72706.6	145435	323
-0.61	0.010	+			0.013					1.475								11	-72707.3	145437	325
-0.53	0.010	+								1.438							+	13	-72705.9	145438	326
0.98	0.010	+												+				11	-72921.0	145864	752
-0.22	0.010	+											1.094					10	-72928.1	145876	765
-0.22	0.010	+					0.151						1.077					11	-72927.7	145877	766
-0.21	0.010	+		0.117									1.076					11	-72928.2	145878	766
-0.22	0.010	+				-0.118							1.098					11	-72928.7	145879	767
-0.22	0.010	+						0.087					1.080					11	-72928.9	145880	768
-0.22	0.010	+	0.050										1.092					11	-72929.1	145880	768
-0.22	0.010	+			0.035								1.084					11	-72930.0	145882	770

Int	dbh	fate	fse	fmo	fmi	afse	afmo	afmi	ri	pri <sup>2</sup>	ry02	pry0 <sup>2</sup>	ryi	pryi <sup>2</sup>	tsfse	tsfmo	tsfmi	df	logLik	AICc	ΔAIC
1.11	0.010	+													+			12	-72969.2	145962	850
1.10	0.010	+														+		12	-72973.8	145972	860
1.21	0.012	+															+	12	-72999.4	146023	911
1.03	0.010	+		0.236														10	-73032.0	146084	972
1.03	0.010	+					0.272											10	-73032.4	146085	973
1.03	0.010	+						0.192										10	-73033.8	146088	976
1.04	0.010	+			0.115													10	-73035.2	146090	978
1.06	0.010	+																9	-73037.5	146093	981
1.06	0.010	+	0.208															10	-73037.3	146095	983
1.06	0.010	+				0.052												10	-73038.3	146097	985
1.52	0.011																	8	-73070.8	146158	1046

**Table S8: Candidate statistical models for counts of recruits (stems ha<sup>-1</sup> y<sup>-1</sup>) between visit intervals using the negative binomial family in R package glmmTMB. Italicised rows are zero-inflation models and bolded are poisson alternatives. An offset log(plot area (ha)\*length of interval (years)) was applied in all candidates for area-specific, annualised predictions.**

Int	off	ri	ryi	ry0	fmi	fmo	fse	afmi	afmo	afse	tsfmi	tsfmo	tsfse	df	logLik	AICc	Δ
0.05	+		1.09			0.20								9	-1086.2	2190.7	0
0.08	+		1.11											8	-1087.4	2191.0	0.28
0.08	+		1.12				-0.23							9	-1086.6	2191.5	0.79
0.04	+		1.10					0.22						9	-1086.6	2191.6	0.85
0.08	+		1.12						-0.29					9	-1086.7	2191.8	1.03
<i>0.02</i>	+		<i>1.18</i>											<i>10</i>	<i>-1085.9</i>	<i>2191.9</i>	<i>1.20</i>
0.06	+		1.14		-0.07									9	-1087.1	2192.5	1.81
0.01	+		1.16								+			11	-1085.1	2192.6	1.84
0.07	+		1.14				-0.09							9	-1087.1	2192.8	2.05
0.12	+		1.09										+	11	-1086.3	2195.0	4.26
0.02	+		1.11									+		11	-1086.6	2195.5	4.81
<i>0.79</i>	+	<i>0.50</i>												<i>10</i>	<i>-1090.3</i>	<i>2201.0</i>	<i>10.0</i>
0.84	+	0.40				0.20								9	-1092.6	2203.5	12.5
0.86	+	0.43												8	-1093.7	2203.6	12.6
0.82	+	0.42						0.23						9	-1092.9	2204.1	13.1
0.88	+	0.43					-							9	-1093.2	2204.8	13.7
						0.18											
0.88	+	0.43								-				9	-1093.3	2204.9	13.8
										0.24							
0.86	+	0.45			-									9	-1093.5	2205.3	14.2
				0.07													
<i>0.84</i>	+	<i>0.46</i>												<i>10</i>	<i>-1092.5</i>	<i>2205.4</i>	<i>14.4</i>
0.86	+	0.43						-						9	-1093.7	2205.6	14.6
							0.04										
0.84	+	0.44									+			11	-1092.0	2206.4	15.4
0.93	+	0.41											+	11	-1092.5	2207.4	16.4
0.84	+	0.42										+		11	-1093.4	2209.2	18.2
1.18	+			0.16										8	-1098.3	2212.8	21.8
<b>0.32</b>	+		<b>1.02</b>											<b>9</b>	<b>-1214.3</b>	<b>2446.8</b>	<b>255.8</b>
<b>0.91</b>	+	<b>0.24</b>												<b>7</b>	<b>-1341.1</b>	<b>2696.3</b>	<b>505.3</b>

### Section 3: Statistical models - additional visualisation graphics

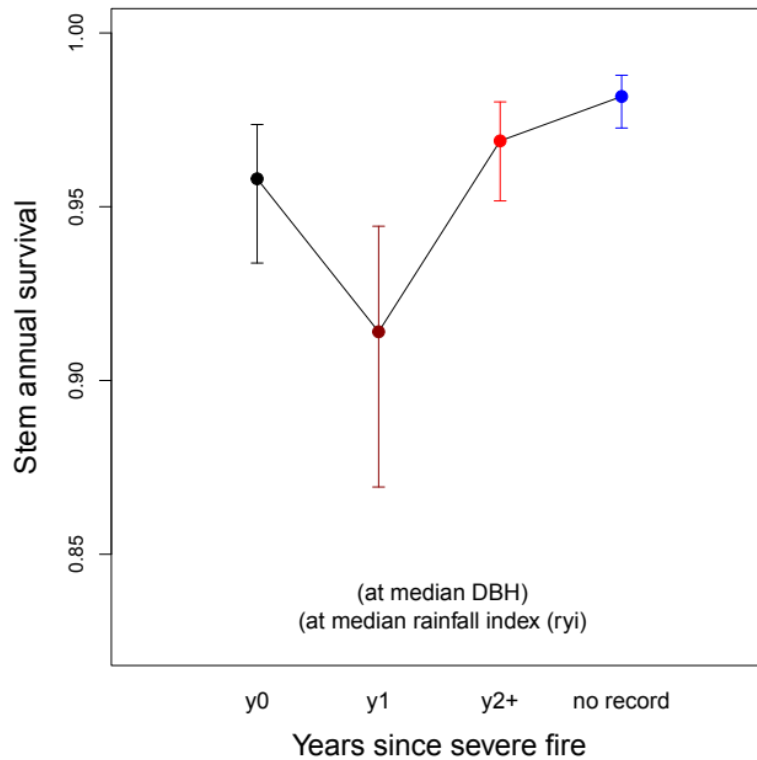


Fig. S1: Predicted values ( $\pm$  95% CIs) for annual stem survival after exposure to severe fire, grouped by years elapsed between the most recent severe fire to the end of each observation interval. The “no record” category is observations from plots where there was no record of severe fire during the study or since the stem entered the observed population. Lowest annual survival is observed the year after a fire (y1) rather than in the year of the fire (y0). All year 0 fires occurred in the year of the visit at which stem status was recorded but before the visit.

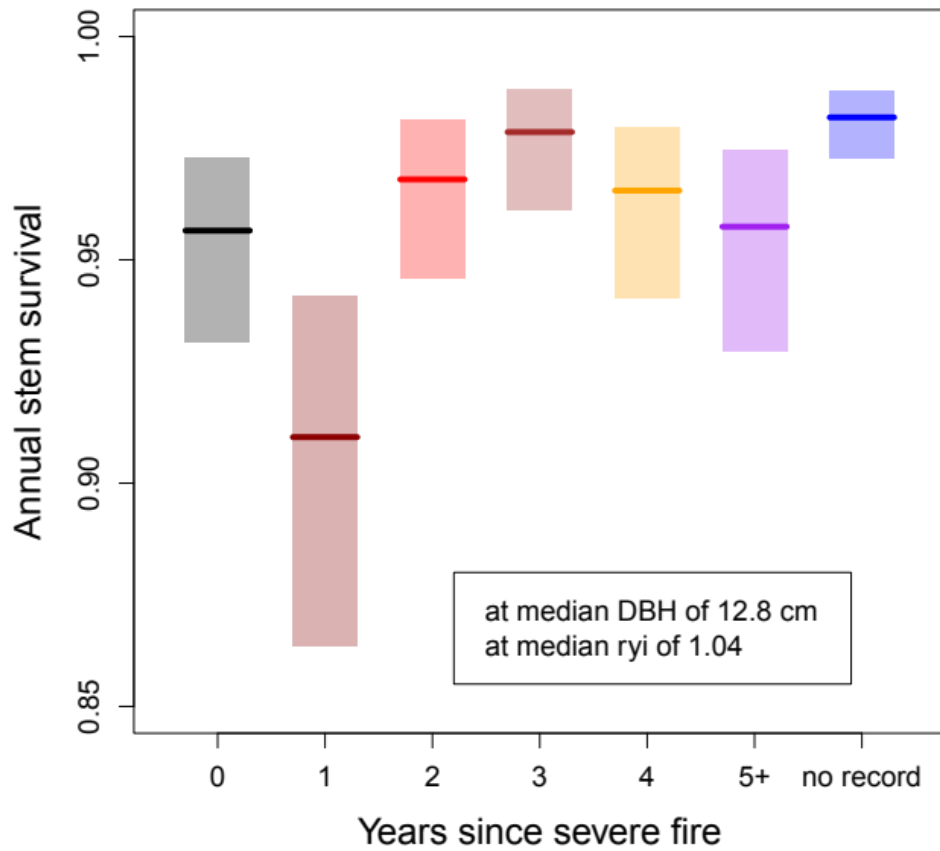


Figure S2: Predicted values ( $\pm$  95% CIs) for annual stem survival grouped by years elapsed between the most recent observation of severe fire to the end of observation interval. The “no record” category is observations from plots where there was no record of severe fire during the study or since the stem entered the observed population. All year 0 fires occurred before the visit at which stem status was recorded.



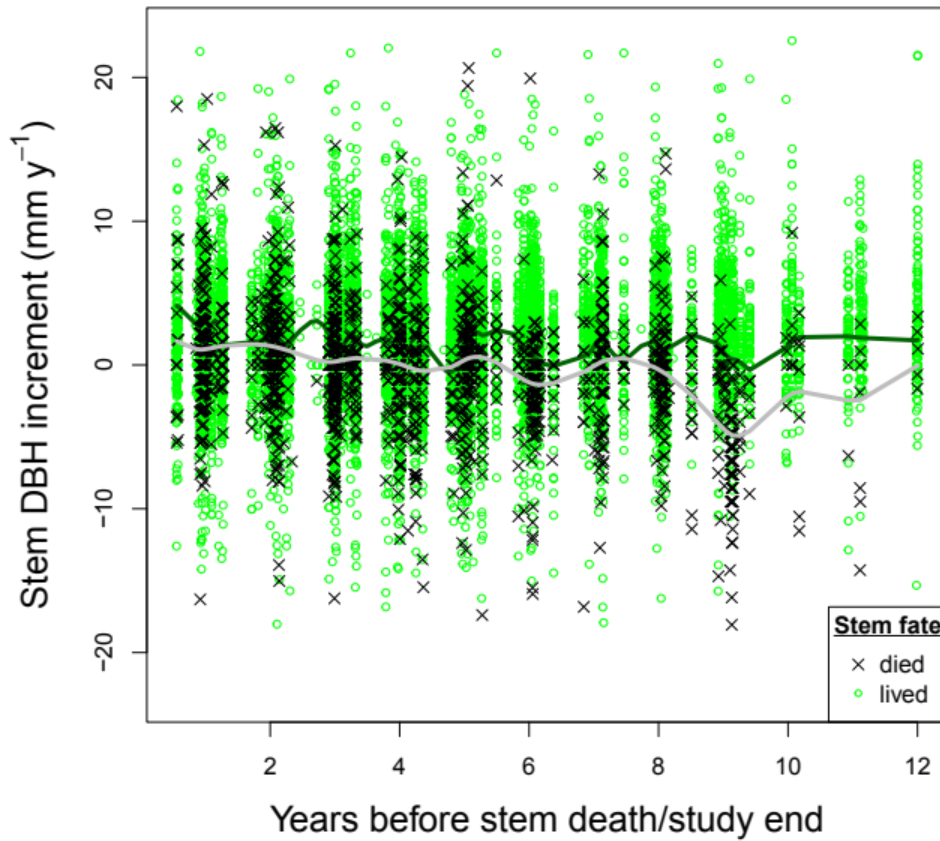


Fig. S3: Comparison of annualised stem increment (between consecutive visits) in trees that died (n=424) and those that were alive at the end of the study. Solid lines are smoothed splines (spar=0.9) for stems that lived (dark green) and those that died (grey). It should be noted that the particular stems comprising the samples changed as stems left the population.

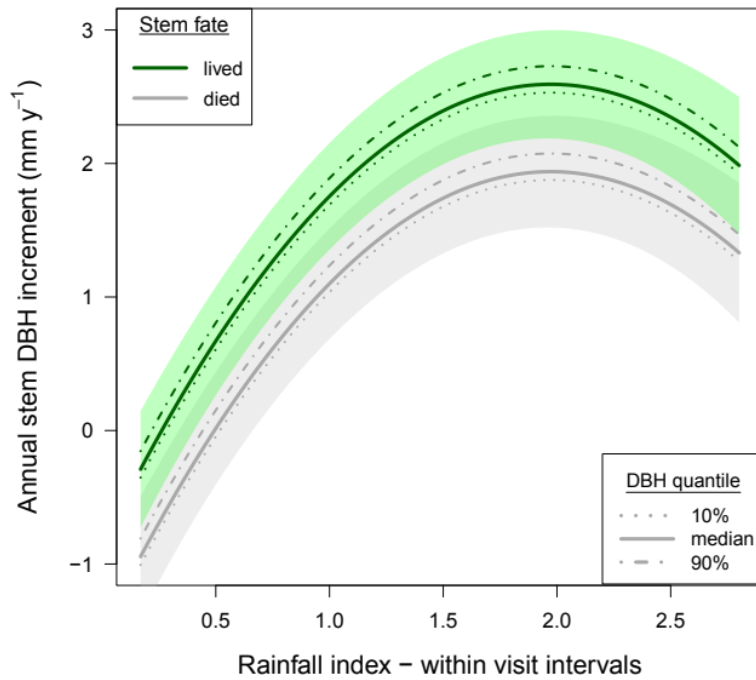


Fig. S4: Predicted stem increment as response to index of rainfall variability (ratio of observed to long-term average) within observation intervals ( $\mathbf{ri}$ ) and fate of stems (died later during the study or survived to study end). Solid lines (with shaded 95% CIs) show predictions at median DBH ( $\sim 12.8$  cm) and dotted lines examples of difference in growth rates at smaller (dotted: 10% quantile  $\sim 6.4$  cm) and larger stem sizes (dashed: 90% quantile  $\sim 27$  cm). DBH effects are relatively minor. Parameter values are in Table 6.

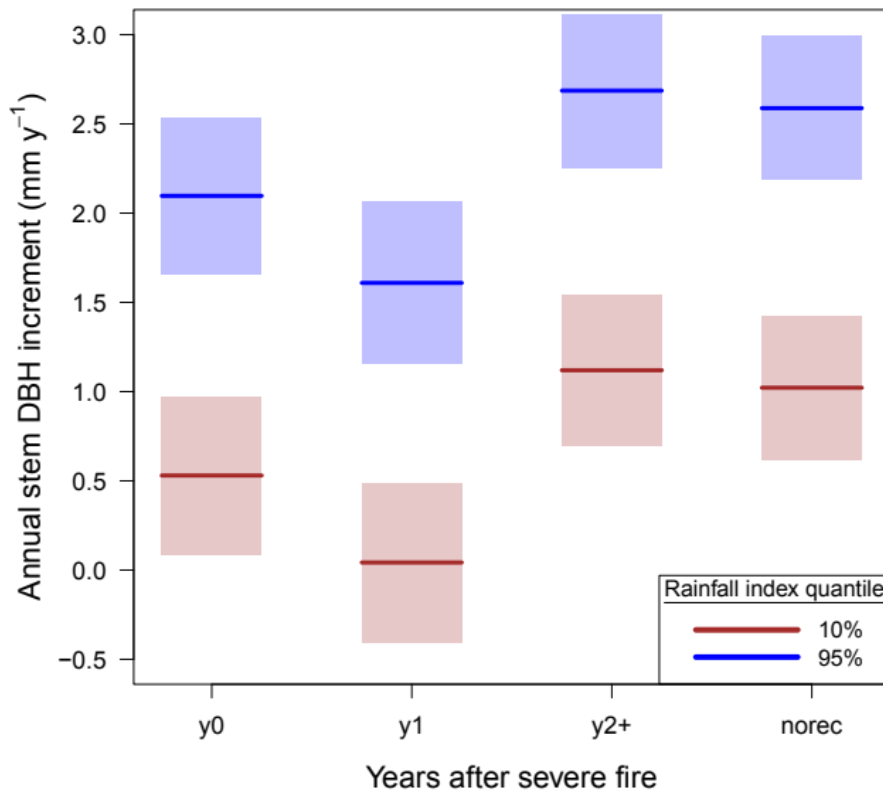


Fig. S5: Predicted stem DBH increment (mean  $\pm$  95%CI) in stems that lived through the study with time since severe fire in relevant plots, including no record of prior exposure, shown with two levels of rainfall variation within intervals: dry, (10% percentile=0.64) and very wet (near peak increment at 95% percentile=1.84). Increments about 0.65 mm y<sup>-1</sup> lower in all time-since-fire categories. Data exclude observations from intervals during which the stem died, and so relate exclusively to stems that lived beyond the years-since-fire categories. Exclusion of death-interval observations arguably results in under-estimation of negative severe fire effects on growth.

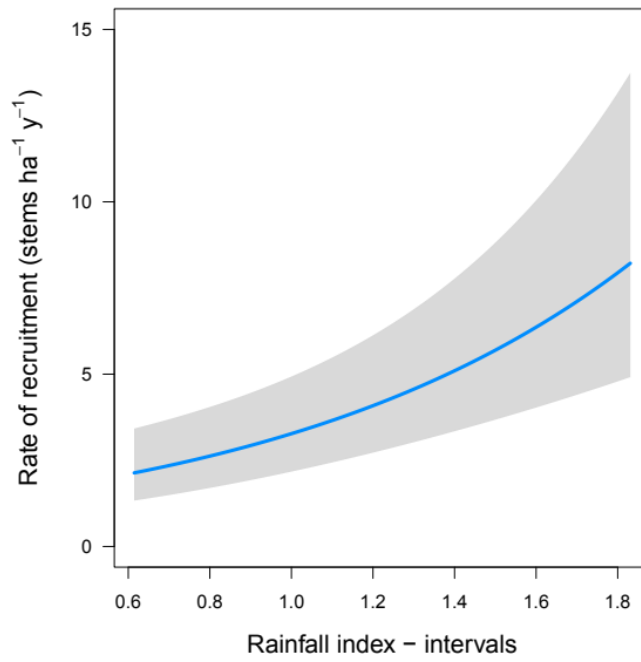


Fig. S6: Predictions (with 95% CI) of rate of addition of recruits (live stems ha<sup>-1</sup> y<sup>-1</sup>) reaching DBH>5 cm during an observation interval in relation to an index of prior rainfall (**ryi**=mean ratio of full rain-years in visit intervals to long term plot mean annual rainfall).

## Section 4: Simulations - additional graphics

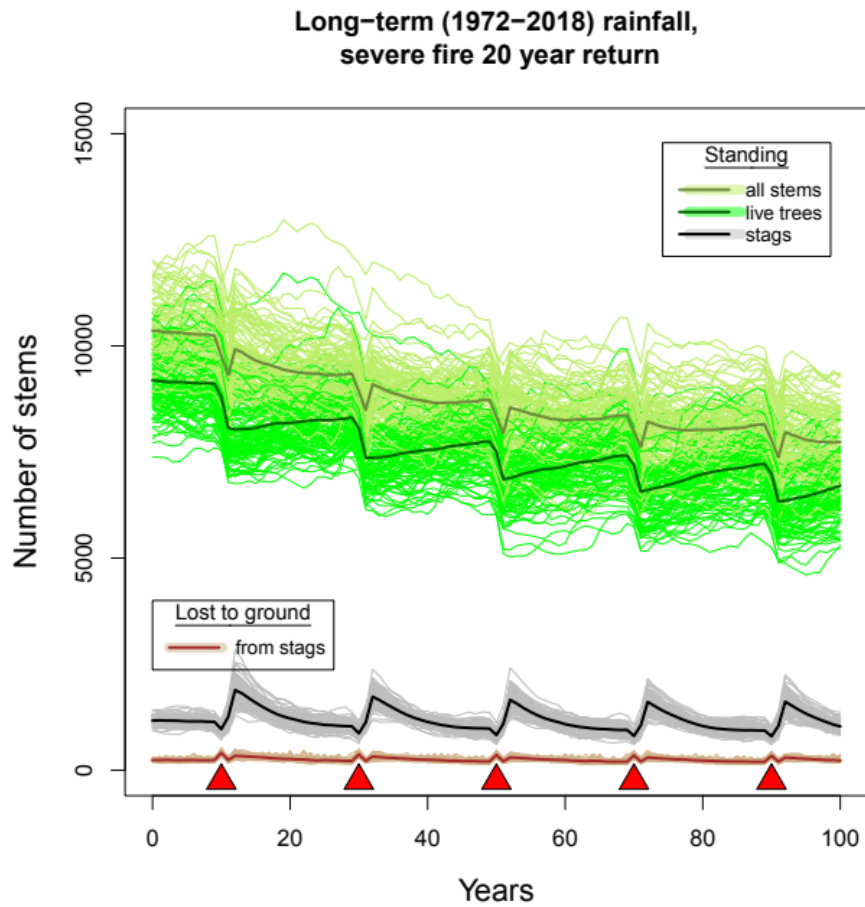


Fig. S7: Simulated change in stem numbers (from a starting population of 10000 live stems) over 100 years in number of standing stems after a 50 year run-up (with no fire). Annual rainfall was randomised at each time step by random picks from samples used in deriving the long-term mean. Lighter, coloured lines show outputs for all of 100 individual simulations including model uncertainty and the heavier lines the means of those simulations. Red symbols on the x-axis indicate the timing of simulated severe fires in the 100 time steps after a 50-year run-up with no severe fire. The apparent post-fire increase in total numbers of standing stems immediately after fire is mostly due to the addition of stags lagging mortality by one time step.

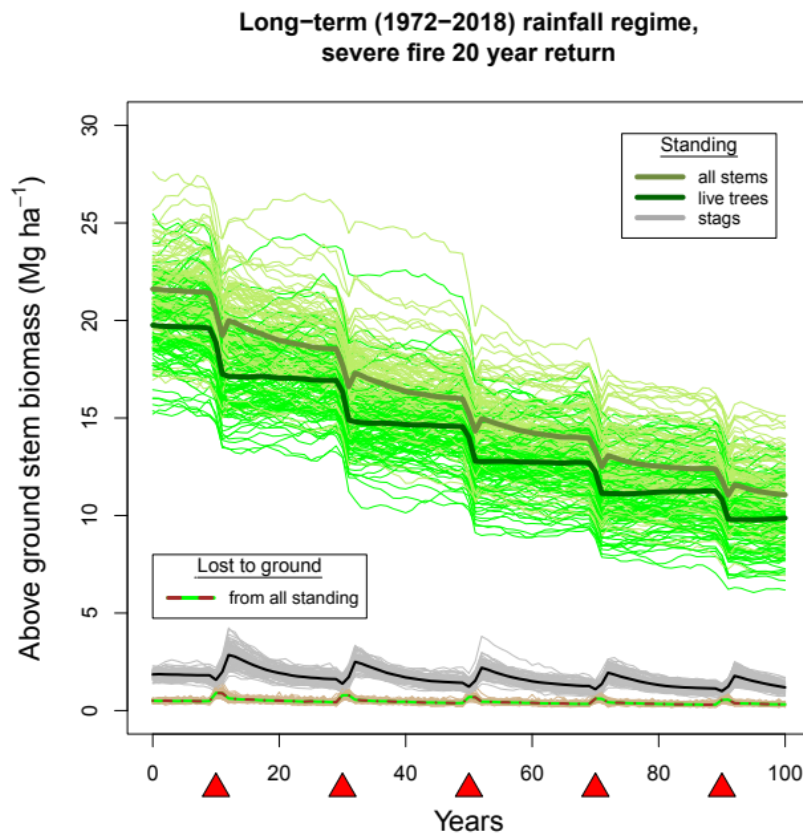


Fig. S8: Simulated change over 100 years in above ground tree biomass ( $> 5\text{cm DBH}$ ) after a 50 year run-up with no fire. Annual rainfall was randomised at each time step within the long-term mean. Lines and symbols as in Fig. S7. AGB losses include shedding of leaves and smaller branches (assumed 50% of branch biomass) at tree death as well as loss (collapse or consumption) of stags. The apparent post-fire increase in total standing AGB immediately after fire is mostly due to the addition of stag AGB to simulation outputs lagging mortality by one annual time step. Live stem AGB reduction with recurring severe fire is more acute than declines in stem numbers because average stem sizes are smaller as recruits replace larger stems lost to fire-related mortality.

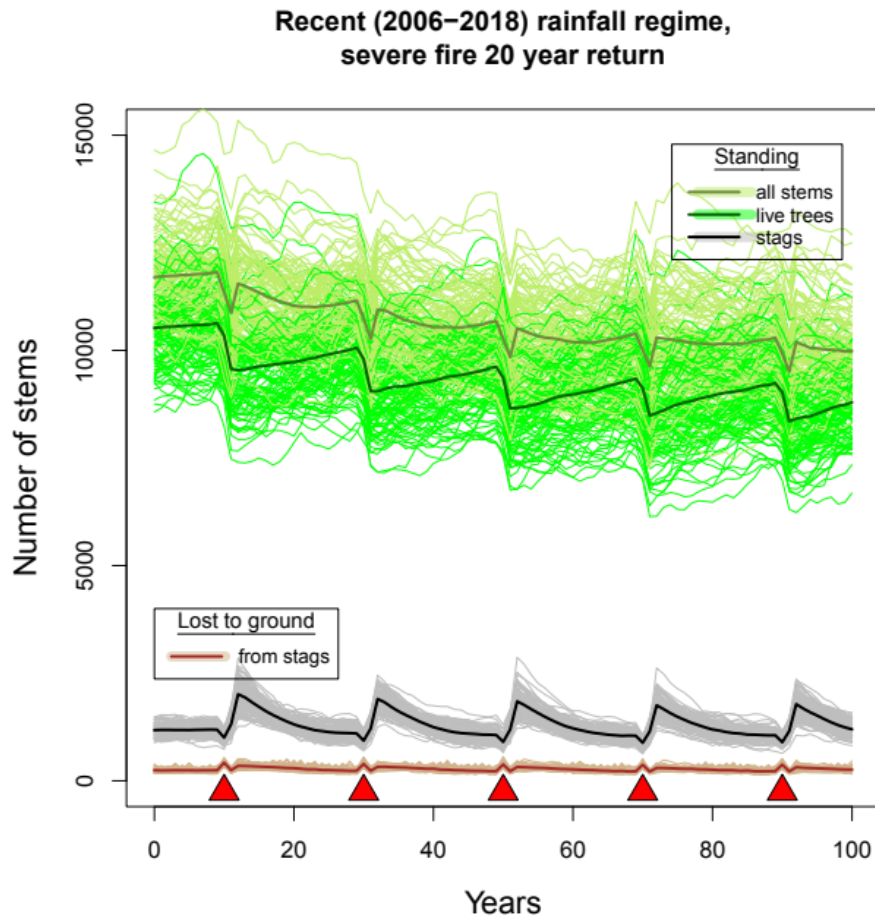


Fig. S9: Simulated change in stem numbers (from a starting population of 10000 live stems) over 100 years in number of standing stems after a 50 year run-up (with no fire). Annual rainfall was randomised at each time step by random picks from samples used in deriving the recent (study period) mean. Lighter, coloured lines show outputs for all of 100 individual simulations including model uncertainty and the heavier lines the means of those simulations. Red symbols on the x-axis indicate the timing of simulated severe fires in the 100 time steps after a 50-year run-up with no severe fire. The apparent post-fire increase in total numbers of standing stems immediately after fire is mostly due to the addition of stags lagging mortality by one time step.

Recent (2006–2018) rainfall regime,  
severe fire 20 year return

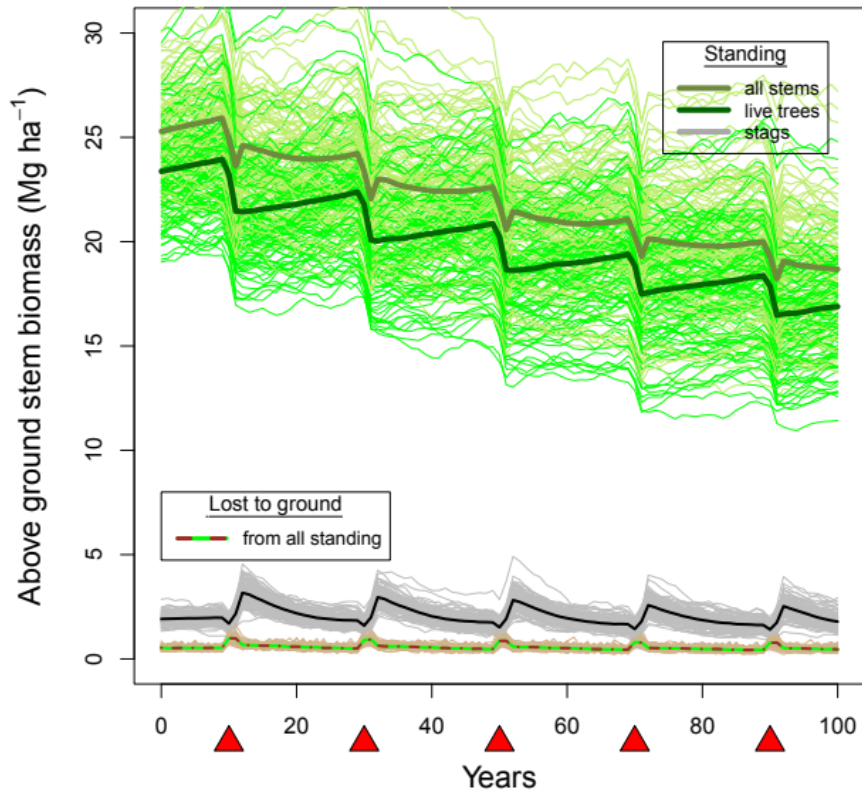


Fig. S10: Simulations (100) all over 100 years of AGB applying recent (study period), slightly above average rainfalls and 5 evenly separated severe fires (frequency=0.05). Fires cause an acute decline in simulated live AGB and a smaller spike in stag AGB. The apparent slight recovery in all standing AGB one year after fire is an artefact of the annual time step and new stag AGB not entering simulations until the year after fire. Recovery of live AGB (dark green solid line) from fire under more favourable rainfalls is partially offset by faster losses of stag AGB.



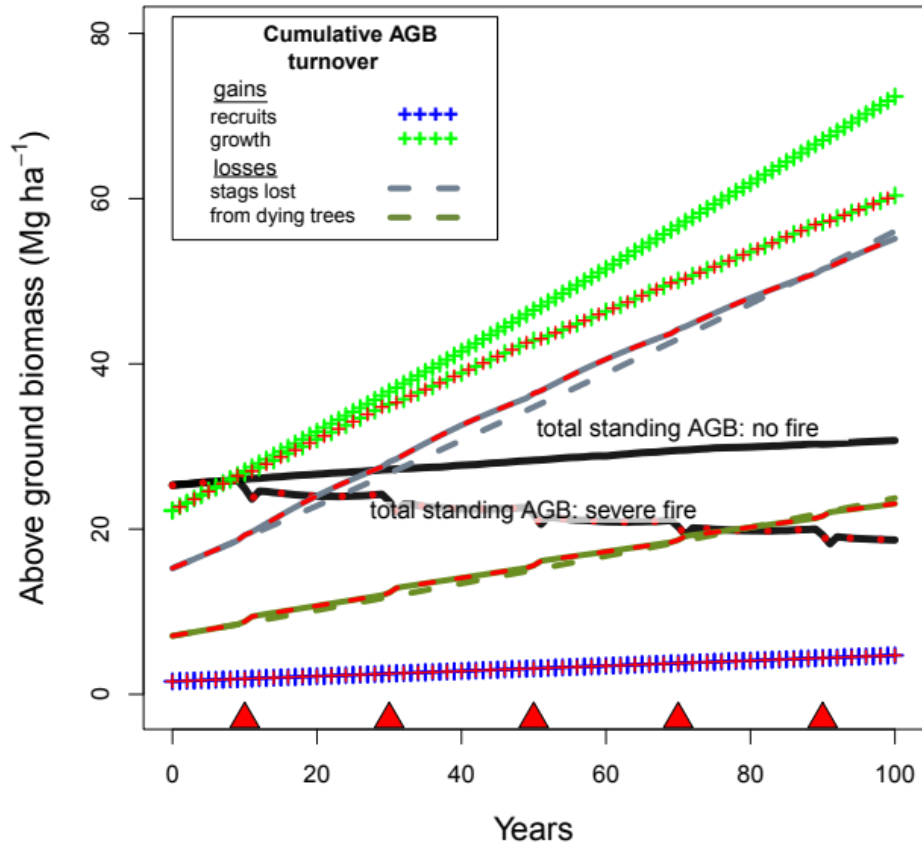


Fig. S11: Simulated cumulative inputs and losses in the absence of severe fire compared with 5 severe fires evenly spread in time (lines or symbols include red elements), under the recent (study-period) rainfall regime, illustrating the relative influence of the contributing statistical models. Despite short term pulses at and shortly after fire incidence, longer-term AGB losses to the ground show modest change in the presence of severe fire. Given the statistical models used, long-term fire-related reductions in simulated standing AGB are mostly attributable to reductions in aggregate inputs from growth by fewer live stems.

Recent (2006–2018) rainfall regime, severe fire 20 year return

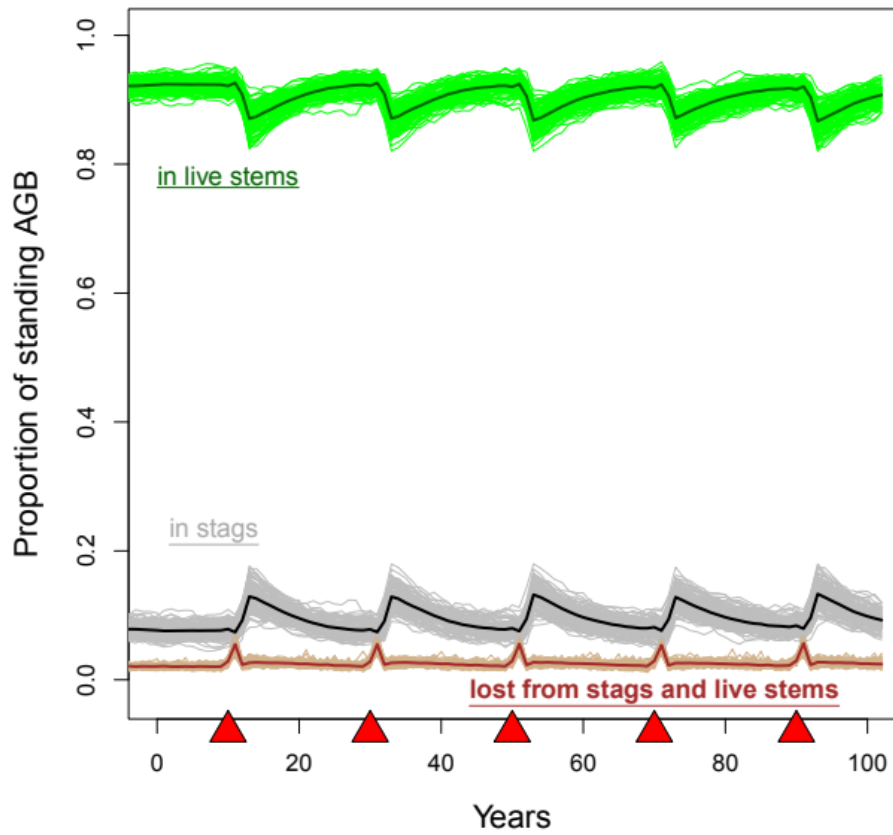


Figure S12: Simulated change over 100 years in proportion of above ground biomass (> 5cm DBH) in live stems, standing dead stems (stags) and lost to the ground. Despite substantial reductions in total biomass (Fig. S10) the simulated proportion of standing biomass in live stems is relatively stable after recovery from the immediate and (relatively short-term) lingering effects of severe fire. The proportion of standing AGB in stags varies substantially with time since last severe fire.

Long-term (1972–2018) rainfall, severe fire average 10 year return

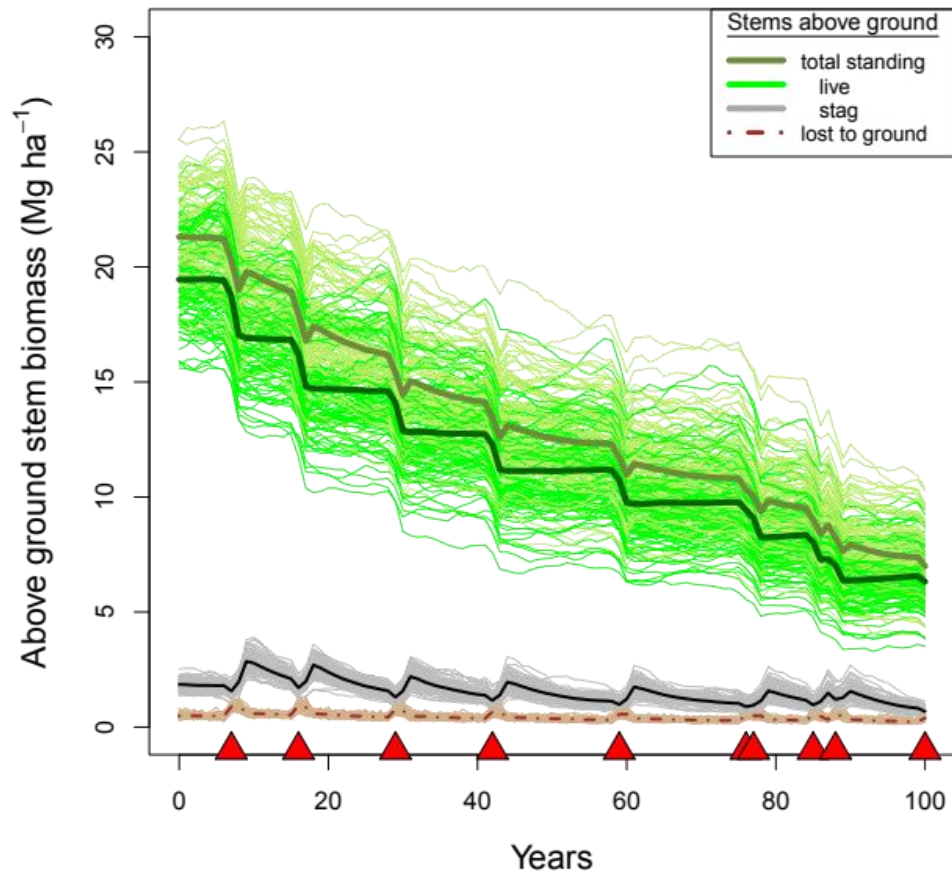


Figure S13: Simulated change over 100 years in proportion of above ground biomass (> 5cm DBH) in live stems, standing deads stems (stags) and lost to the ground under a regime of severe fire about half the return time found in this study. The sequence of 10 fires was randomised.

Long-term (1972–2018) rainfall regime,  
10 severe fires random timing

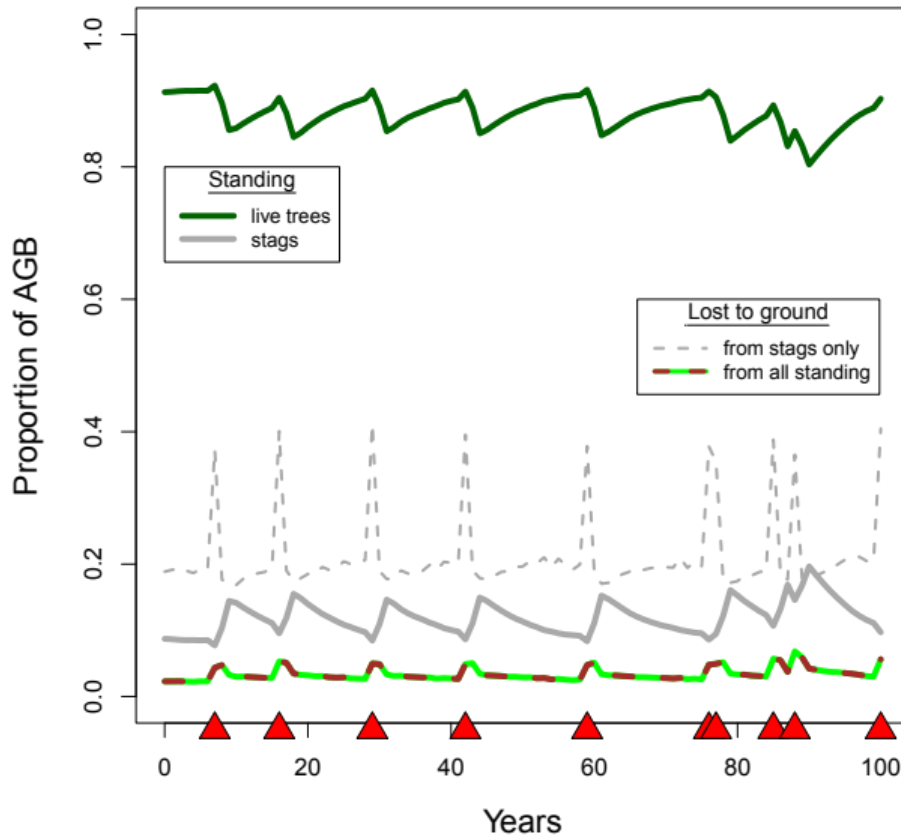


Figure S14: Simulated change over 100 years in proportion of above ground biomass (> 5cm DBH) in live tree stems, standing dead stems (stags) and lost to the ground under a regime of severe fire at about half the return time found in this study. The sequence of 10 fires was randomised. The proportion of biomass in stags is substantially increased overall and especially a few years after fire occur, while live biomass falls by over 60% (Fig S13). Loss of biomass from stags peaks strongly immediately after fires but losses are more than compensated by gains from new mortalities under high frequency severe fire.

Recent (2006–2018) rainfall regime,  
10 severe fires random timing

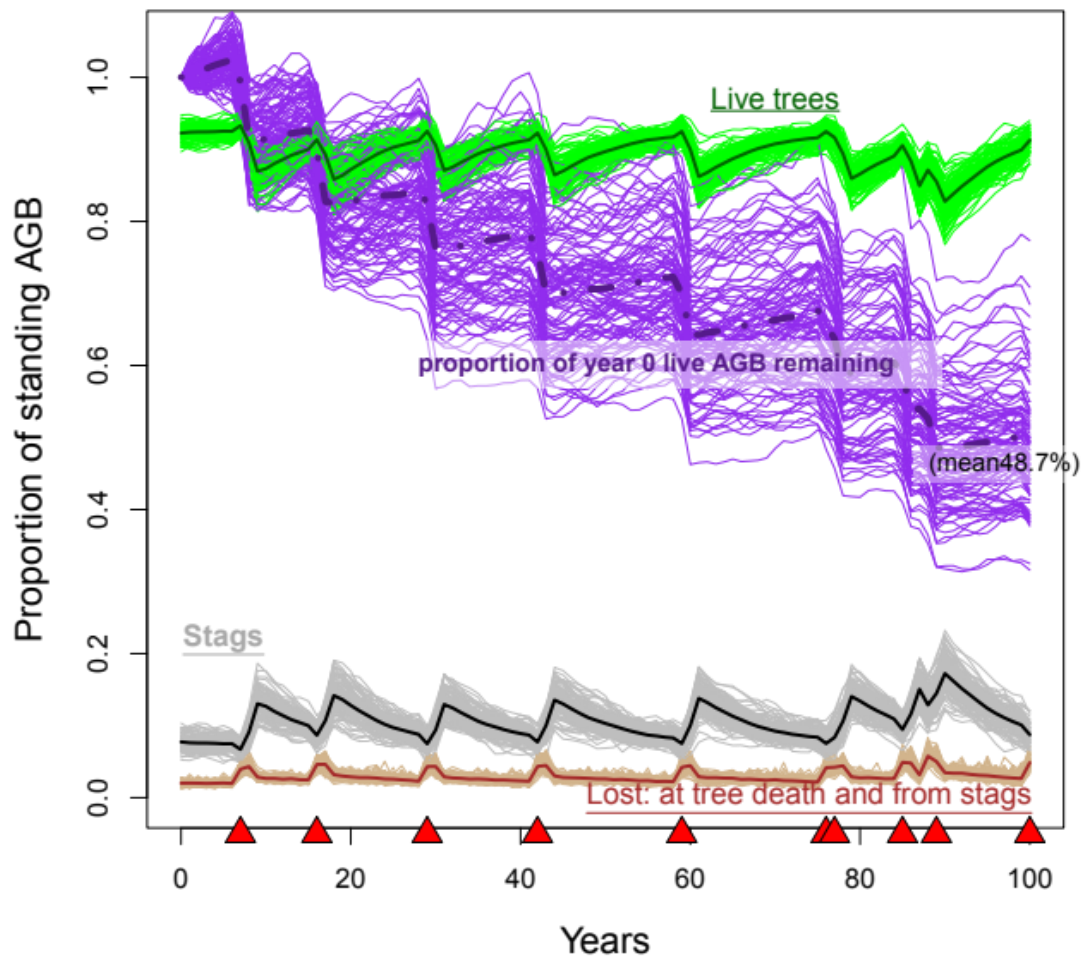


Figure S15: Simulation of changes in relative representation (proportion) of live tree stem and stag AGB in total standing AGB under a high frequency severe fire regime ( $0.10 \text{ fires y}^{-1}$ ) with randomly selected timing. Between short term peaks soon after fires, contributions of stags to standing AGB show limited increase, despite the very substantial suppression of live AGB (purple lines) by more than 50% averaged over all simulations. Under drier conditions (simulating observed long term mean), live AGB at year 100 is 32.5% of the year 0 level.

Comparing live AGB trajectories  
two rainfall regimes and 4 fire histories

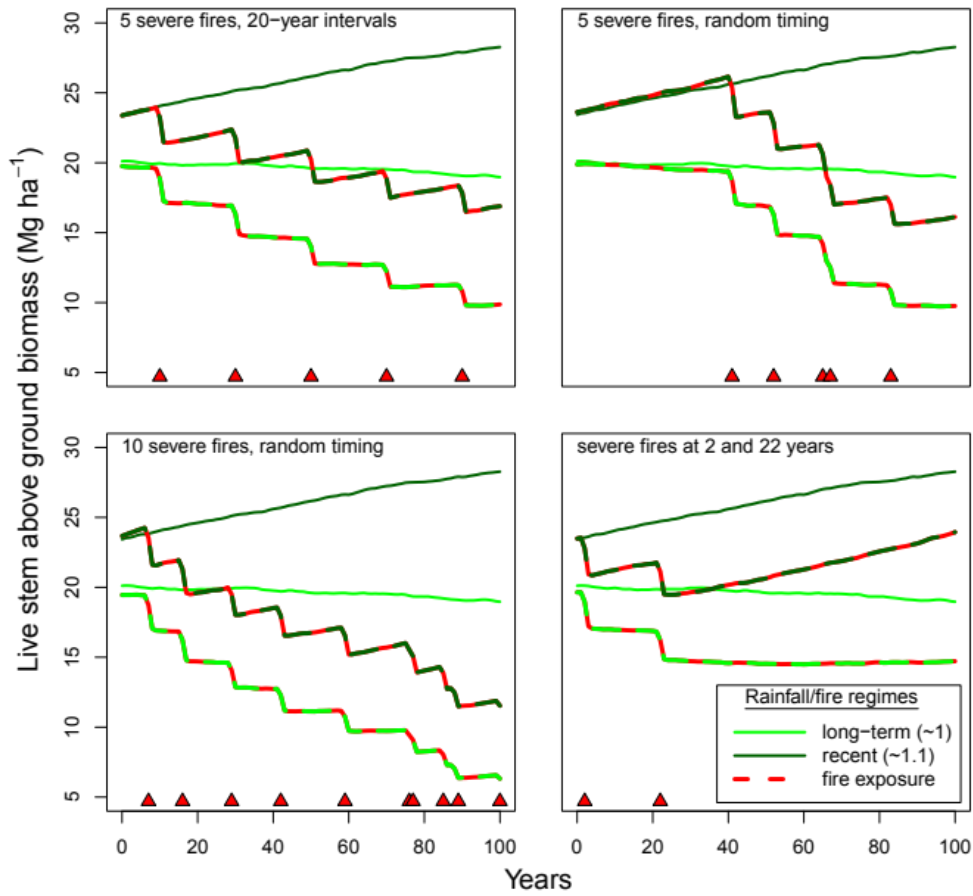


Fig. S16: Summary of simulations of 100-year changes in live stem AGB specifying different rainfall (average long-term vs. recent (higher) rainfalls and fire frequency and timing. Panel 4 illustrates the long-term consequences of relatively few severe fire exposures, notably very slow recovery at long-term average rainfalls compared with more recent rainfall regimes.

Comparing trajectories of AGB loss from standing stems  
two rainfall regimes and 4 fire histories

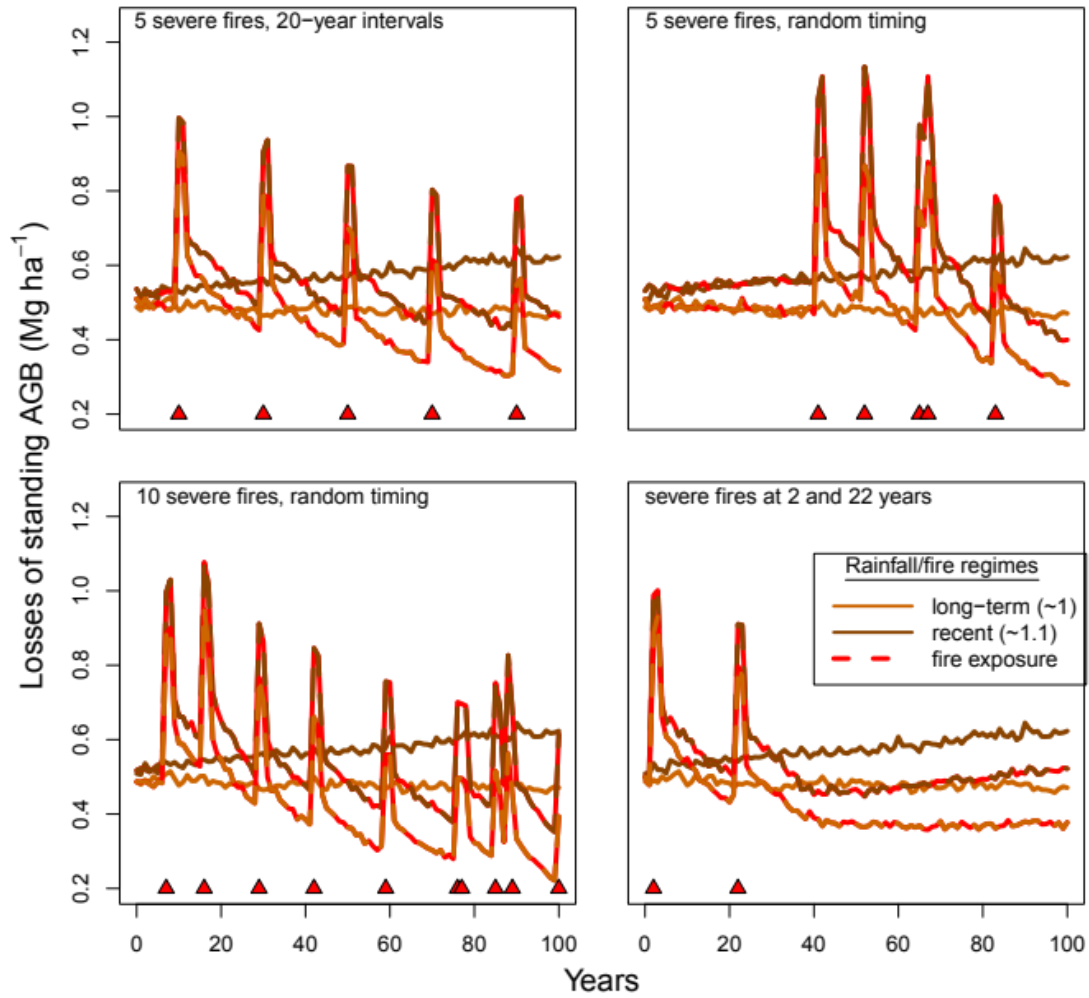


Fig. S17: Simulations of AGB loss from standing stems. Spikes in losses with fire include both the immediate (same year) loss of existing stags and branches assumed to be lost from live trees on increased mortality in the year of fire and in the two years following.

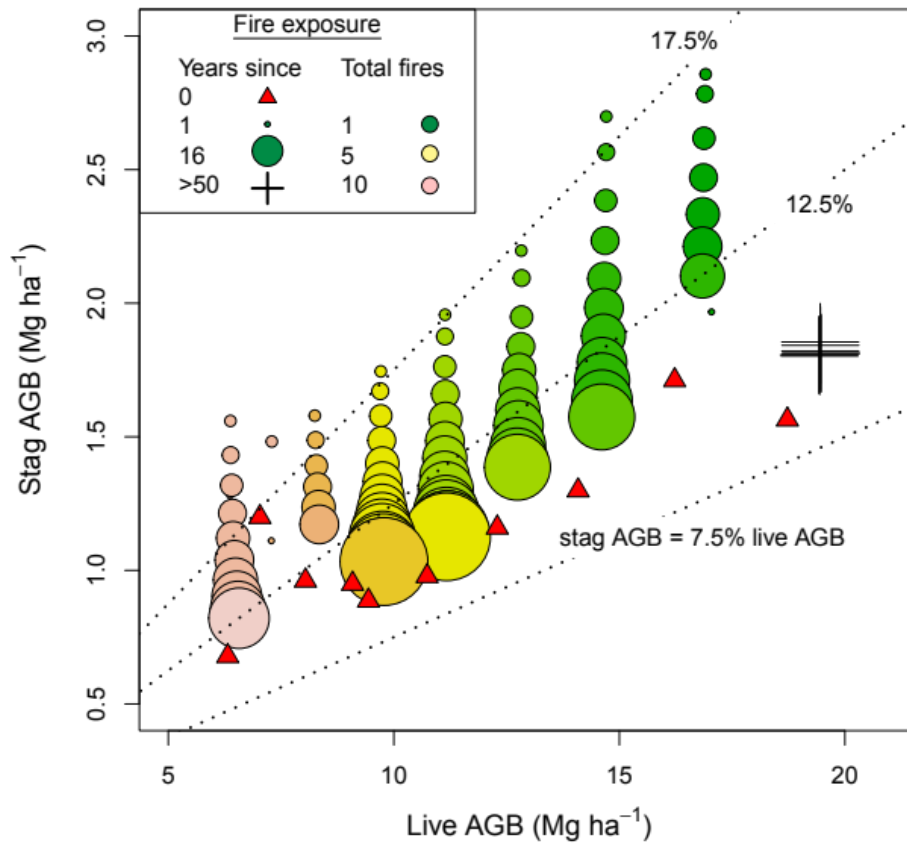


Fig. S18: Simulations (mean of 100) of relationship between AGB of live trees and of stags with 10 severe fires in 100 years and under long-term rainfall regimes randomised at each time step. Over the longer term, repeated severe fires substantially lower both live AGB and stag AGB, but see a slight increase in proportion of standing AGB in stags. Absolute and relative stag AGB decline with time since last severe fire (larger circles=longer time since fire in range 1 to 16). A single observation of a fire-year is obscured.



## Section 5: Simulations- additional graphics on sequestration performance

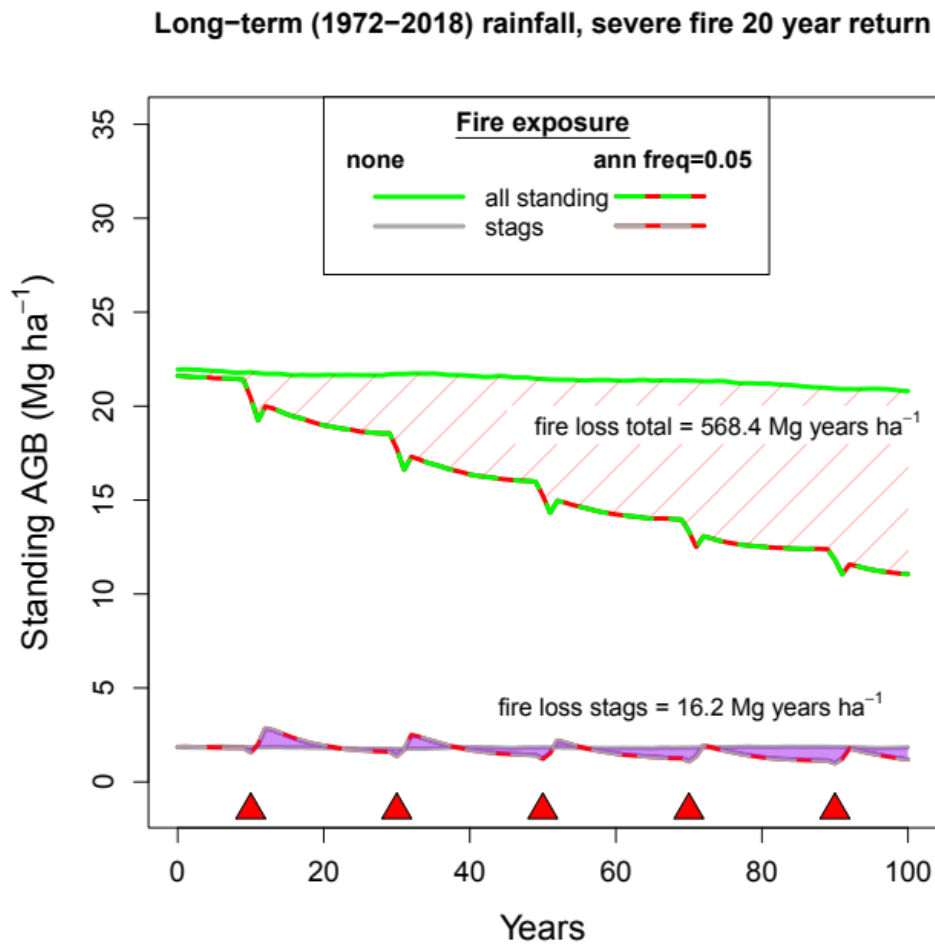


Fig. S19: Simulation of changes in total standing AGB and stag AGB shown separately. Over the whole simulation period, the projected net losses in stag biomass due to severe fire (purple polygons) are 2.9% of reductions in live biomass. In the 20 years following the first fire, simulations suggest a modest net increase in standing stag biomass ( $4.0 \text{ Mg years ha}^{-1}$ ) compared to a  $53.8 \text{ Mg years ha}^{-1}$  reduction in standing live biomass.

Long-term (1972–2018) rainfall, 5 severe fires random intervals

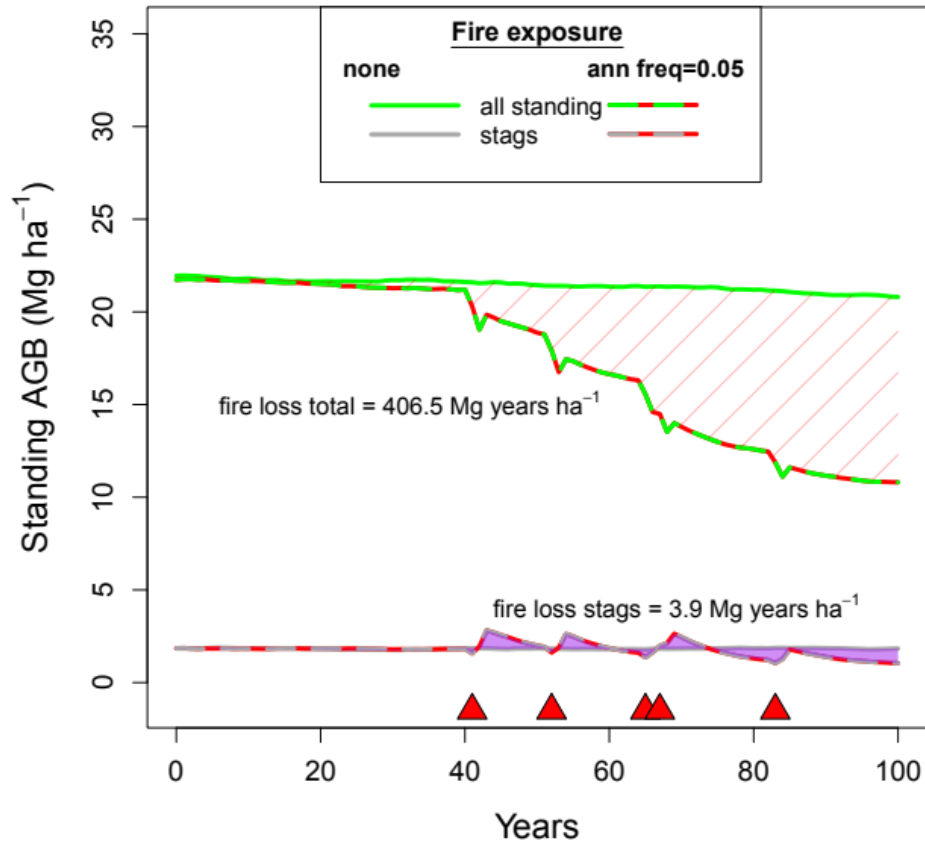


Fig. S20: Simulation of changes in total standing AGB and stag AGB shown separately for 5 randomly-timed severe fires in the 100-year simulation. Over the whole simulation period, the projected net losses in stag biomass due to severe fire (purple polygons) are 1.0% of reductions in live biomass. Slow rates of live biomass recovery from severe fire are associated with lower total losses when first exposure is delayed even at the same total exposure (see also Fig. S21).

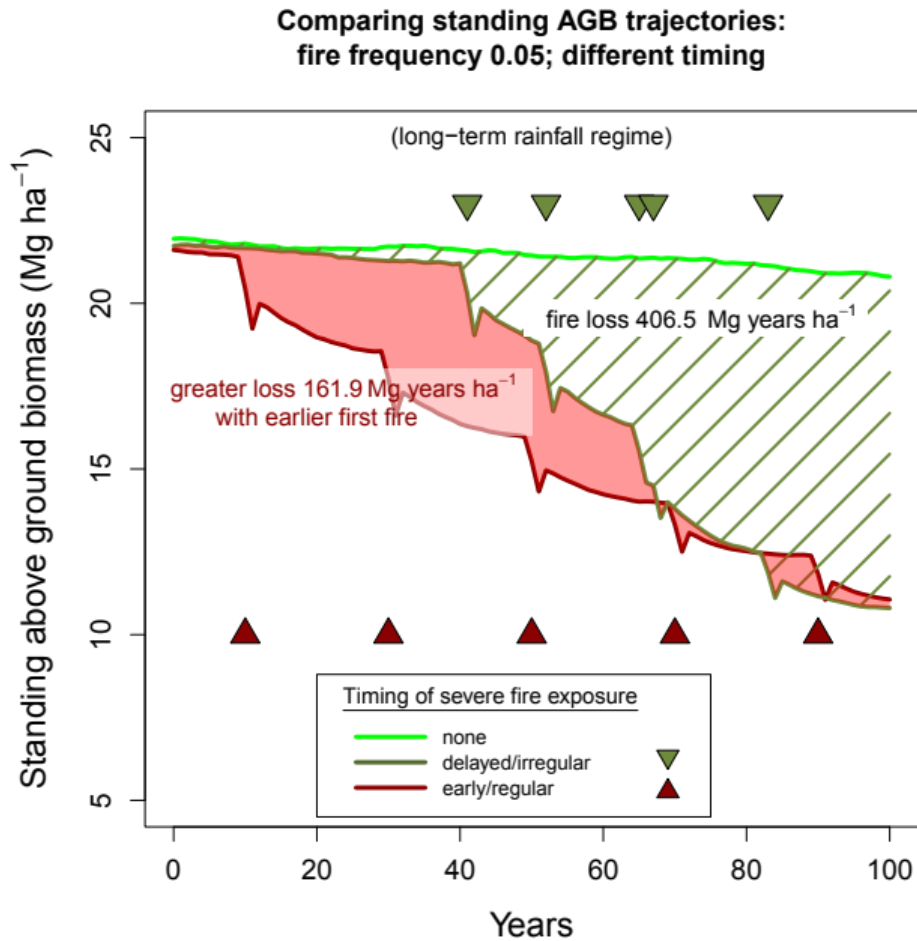


Fig.S21: Comparison of changes in total standing AGB from means of 100 simulations for each of no severe fire, five severe fires at 20 year intervals and with randomly selected fire timing. Over the whole simulation period, aggregate sequestration (in  $\text{Mg years ha}^{-1}$ ) varies substantially with timing of the same number of severe fires, being 39% higher when they begin 10 years into the simulation and recur at 20 year intervals (red triangles) compared with random timing (green triangles) with markedly later onset of severe fire exposure.

Recent (2006–2018) rainfall regime:  
severe fire frequency 0.05; varying timing

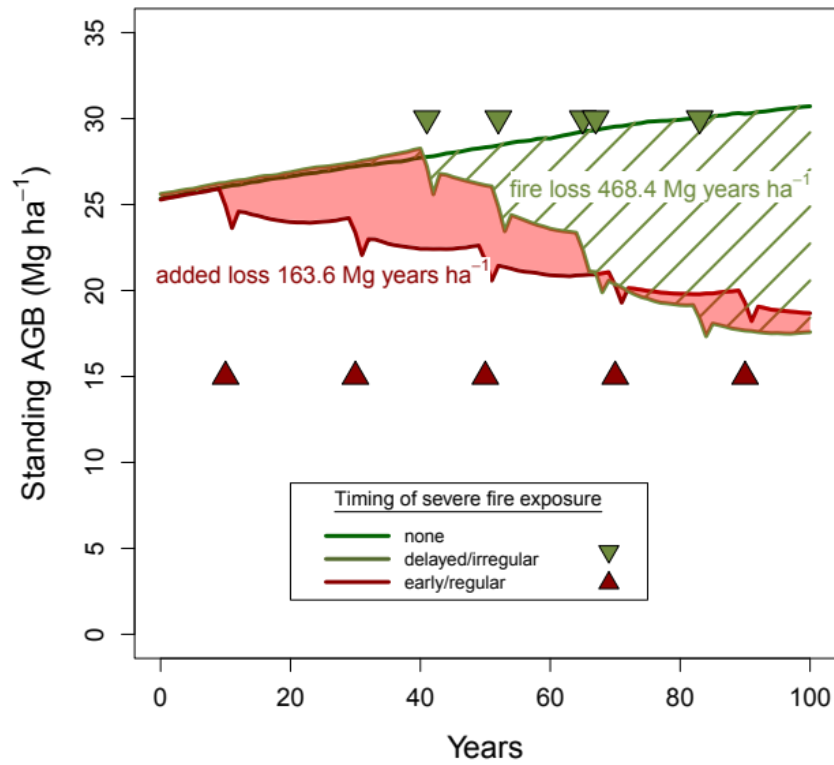


Fig. S22: Simulations comparing changes in total standing AGB with 5 severe fires at 20 year intervals and the same number of randomly timed fires in the 100-year simulation period under the recent (study period) rainfall regime. Aggregate sequestration (in Mg.years.ha<sup>-1</sup>) is 25.9% lower (red shading) when fires start earlier.

Recent (2006–2018) rainfall regime, 10 severe fires random timing

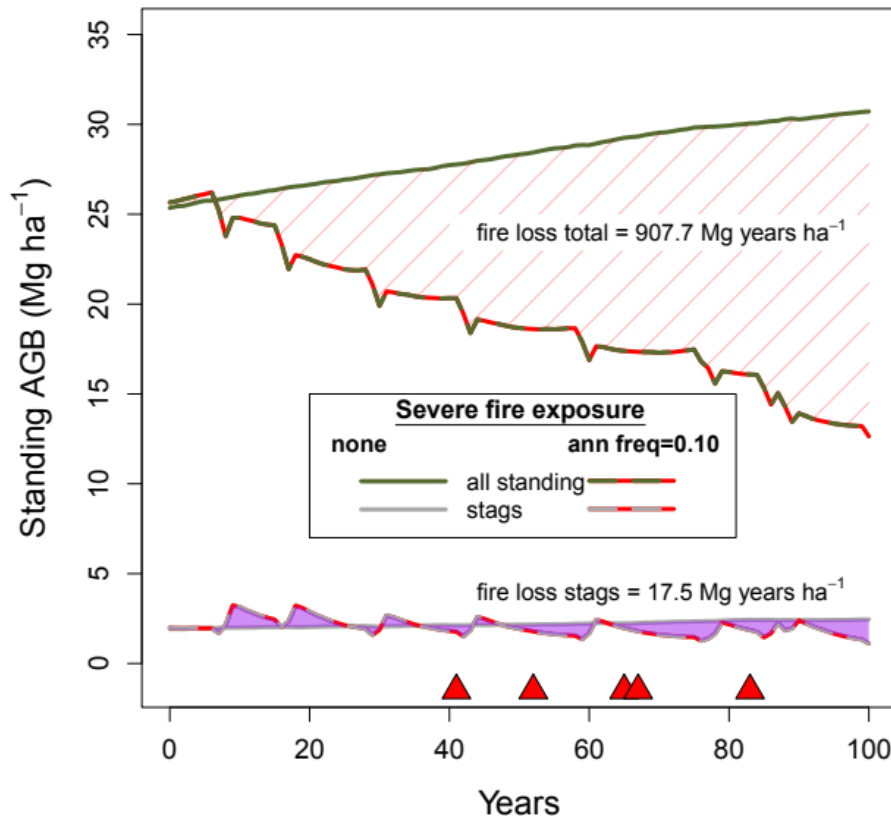


Fig. S23: Comparison of simulated standing AGB trajectories over 100 years in strongly contrasting fire regimes (no severe fires and 10 severe fires) and recent (slightly higher) average rainfalls. Cumulative sequestration is reduced by 32.1%, with net aggregate sequestration in stags also reduced (by 8.0%).

## Section 6: Species differences in stag dynamics

To examine divergence in rates of loss of *dd* and *doa* stems in relation to species of origin, we plotted the relative AGB of stags and live stems pooled across all plots within the hyperspace defined by the random effects intercepts (Fig. S21). There are conspicuous differences in how the *O* *doa* stag population (present at study commencement) scales to living stems. Most obviously, *Callitris intratropica* and *Erythrophleum chlorostachys* comprise much larger proportions of the total stag biomass than of the live population. Less conspicuously, some abundant eucalypts (notably *E. tectifera* and *E. leucophloia*) are relatively better represented in the stag population than the live.

Many species, including *Acacia* and *Grevillea* (right side of plot) make minimal contributions to *doa* standing dead wood even though they collectively present substantial stem mortality (red circles). An obvious departure from this general pattern involves stands of *Grevillea pteridifolia* (labelled Gre pte) and *Acacia* spp. (Aca sp.). Local episodic recruitment and mortality events appear to generate these apparent anomalies. For example, 29 dead stems of *Grevillea pteridifolia* (of 51 in the entire study sample) were found in a single plot at establishment, and all these dead stems had been lost by the second visit to the site.

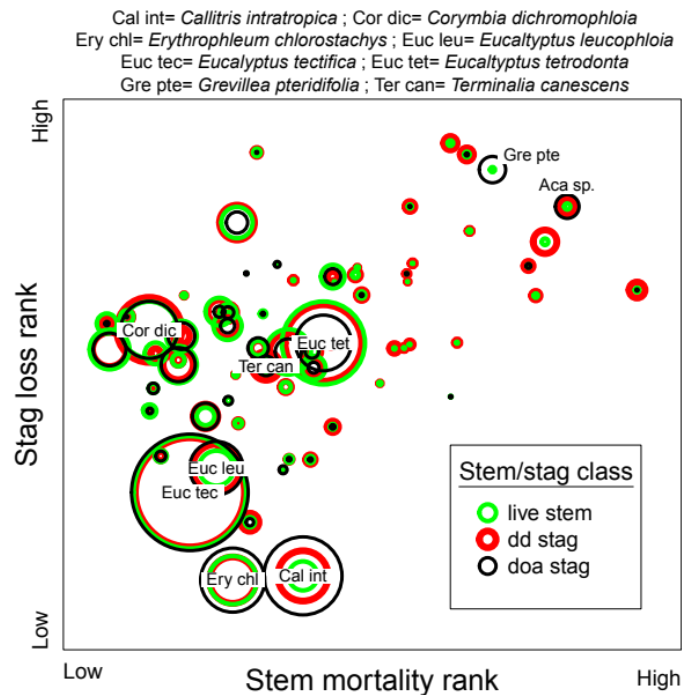


Fig. S24: Stag species positioned by random effect intercepts from models for mortality (x-axis) and stag loss (y-axis). The area enclosed within symbols is proportional to relative AGB within each stem/stag class. Those with larger black circles are better represented within the established stag stands: and those with large *doa* presence relative to the live population (green) and fewer recent stags (red) would appear to provide more resilient stags.

## Section 7: Fire timing and projected sequestration performance

To illustrate the potential effects of timing of severe fire relative to time-bounded (15 year pre-project baseline and 25 year crediting period as presently prescribed in Australian savanna burning assessment methods) sequestration projects, we considered a situation in which active fire management projects reduced severe fire risk from a pre-project annual frequency of 0.05 (return time=20 years) to 0.025 (return time=40 years) in the post-project simulation years. At these frequencies, probability of at least one severe fire in a pre-project baseline period of 15 years is 53.7% and in a 25-year crediting period is 46.9%. We examined by simulations the implications of these relatively common outcomes for assessments of sequestration performance (standing AGB) for projects.

First, to directly examine effects of fire timing on sequestration outcomes, we ran 9 sets of specified severe fire exposures: namely no severe fire in either baseline or crediting period (designated 0,0); one severe fire in either baseline (1,0) or crediting period (0,1); one severe fire in both of the baseline and crediting periods (1,1). These simulations don't directly apply fire frequencies but as noted above, will be commonly observed exposures at the frequencies of interest here. We focused on differences in timing of severe fires by setting them early in the relevant periods (year 3) or late (year 13 for baseline and year 23 for crediting periods). We used random picks from annual study period rainfall observations and exposed all simulations to 3 severe fires in the 60 years prior to project baseline, at years 10,30 and 50. We used the mean of the 10 replicates to characterise each of the nine "project" sequestration outcomes.

Second, based on the assumed underlying fire frequencies of 0.5 pre-project (including the baseline) and 0.025 for the crediting period, we made 10 different random assignments (using R's *rbinom* procedure ) of severe fire events in the 75-years preceding project initiation and in the crediting periods and ran 10 replicates of each of these putative projects.

For both sets of simulations we considered two putative sequestration performance metrics based on (1) comparison of total standing AGB (live and dead) and stag AGB at the beginning and end of crediting periods (2) comparison of cumulative sequestration performance ( $\text{MgAGB}\cdot\text{ha}^{-1}\cdot\text{years}$ ) averaged over the length of the relevant baseline and crediting periods ( $\text{Mg}\cdot\text{ha}^{-1}\cdot\text{y}^{-1}$ ). Results are illustrated in Fig. S25 and summarised in Table S9 below.

Given the strong peaks in stag AGB at the time of fire, neither metric for stag AGB was reliably associated with overall sequestration performance. For total standing AGB (live stems and stags), the four examples of early baseline-period fires were associated with improved crediting period sequestration (3) or modest reduction when followed by crediting period fire (1). For fires late in the baseline period, sequestration performance negative or weakly positive, varying among metrics.

The most extreme simulated reductions in sequestration occurred in the example combining a late baseline period fire with early crediting period fire (Table S9).

**Table S9: Summary of mean sequestration performance of 9 fire management “projects” (10 simulations for each project) to illustrate the effects of fire timing on apparent sequestration performance. Cells shaded in green show simulations that generated putative net simulation benefits: higher average annual AGB during the crediting period than related baseline average or higher standing AGB at the end of the crediting period than at its beginning).**

proj	severe fire exposure		all standing AGB (Mg.ha <sup>-1</sup> )				stag AGB (Mg.ha <sup>-1</sup> )				
	baseline	crediting period	base-	crediting period		base-	crediting period				
			line	annual	annual	start	end	line	annual	annual	start
mean	mean	mean	mean	mean	mean	mean	mean	mean	mean	mean	mean
1	0	0	21.10	22.67	23.16	24.26	1.78	1.86	1.83	1.92	
2	1(early)	0	18.16	18.16	18.50	19.63	2.05	1.54	1.72	1.48	
3	1(late)	0	20.27	20.25	21.41	21.62	1.73	1.84	2.70	1.83	
4	1(early)	1(early)	17.38	16.88	18.45	18.35	1.80	1.54	1.60	1.40	
5	1(early)	1(late)	18.11	18.92	19.44	19.43	1.96	1.55	1.68	2.78	
6	1(late)	1(early)	20.69	17.85	21.27	18.04	1.73	2.02	2.86	1.56	
7	1(early)	1(late)	19.72	20.18	20.58	20.74	1.60	1.80	2.43	2.72	
8	0	1(early)	18.72	18.51	20.16	19.86	1.62	1.76	1.61	1.57	
9	0	1(late)	19.43	20.36	20.92	21.03	1.68	1.67	1.76	2.74	

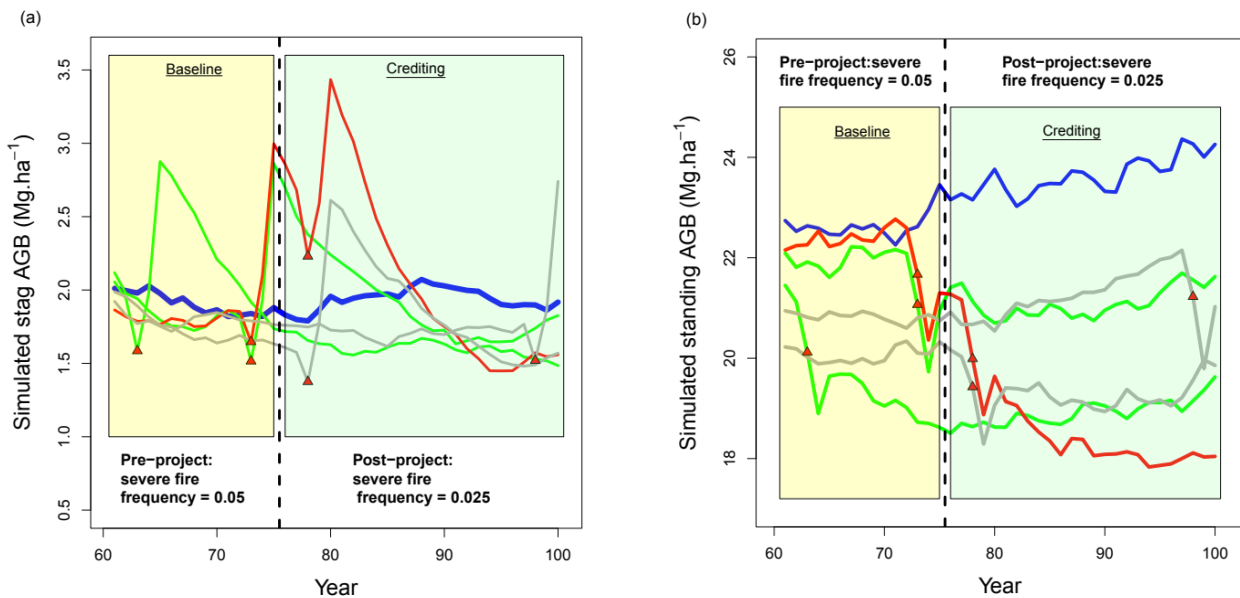


Figure S25: Examples of the effects of severe fire timing on simulated sequestration performance of savanna burning projects summarised in Table S9. In the absence of severe fire stag AGB (a) is relatively stable (blue line). Severe fire in either baseline or crediting periods, especially if repeated (red) generates strong peaks following tree death. Fires at any time in baseline period can depress total



standing AGB (b) through much of the subsequent crediting period, as do fires early in the crediting period itself. Obviously late crediting period fires have less impact on net sequestration performance.

Simulation examples randomised for fire frequency and timing based solely on assumed fire frequency of 0.05 pre-project and 0.025 in crediting periods are summarised in Table S10. Despite the structuring of all of these “project” simulations as successful - in that severe fire risk was halved from inception - the effects of variation in frequency and timing of randomly assigned fire exposure meant that only 5 of 10 generated apparent sequestration benefits. Four of the five “successes” experienced no severe fire during the crediting period and the fifth was exposed in the last year, so that effects were mostly felt after the crediting period.

Fires during the baseline period did not necessarily depress baseline AGB enough to offset fires in the crediting period, especially if they occurred early in the baseline, allowing some recovery by project initiation. None of the projects with fires in both baseline and crediting periods returned an apparent sequestration benefit. As discussed above, benefits in sequestration in stags, even in the otherwise favourable “projects” were more erratic and trivial in scale compared with change in live standing AGB. Fire history prior to the putative 15-year baseline period was important in setting initial AGB from which projects worked. For example, the case (#4) with the most extreme pre-project fire history, AGB at project start was only 52% of the example with no pre-project severe fire exposure.

**Table S10: Summary of mean sequestration performance of 10 fire management “projects” (10 simulations for each project) that successfully reduced annual probabilities of severe fire exposure from 0.05 to 0.025. Cells shaded in green show simulations that generated net simulation benefits: in particular, higher average annual AGB during the crediting period than related baseline average or higher standing AGB at the end of the crediting period than at its beginning).**

	Severe fire exposure		All standing AGB (Mg.ha <sup>-1</sup> )				Stag AGB (Mg.ha <sup>-1</sup> )			
	Pre-project <sup>1</sup>	Project <sup>2</sup>	base- line annual mean	crediting period annual mean	start	end	base- line annual mean	crediting period annual mean	start	end
1	3(-6,-19,-29)	b3,c0	16.85	17.18	17.21	18.85	1.95	1.35	1.51	1.45
2	4(-8,-10,-13,-32)	b5,c7	15.40	14.73	15.79	15.39	1.80	1.39	1.43	1.20
3	3(-8,-12,-32)	b0,c0	19.38	21.49	21.38	23.23	1.58	1.64	1.48	1.86
4	6(-2,-3,-16,-26,-28,-33)	b8,c11	13.39	12.87	13.64	13.35	1.72	1.22	1.31	1.07
5	1(-1)	b0,c0	23.92	25.74	25.88	27.66	2.27	1.95	1.88	2.07
6	0	b3,c23	25.71	25.45	26.23	24.38	2.62	2.05	2.34	2.24
7	1(-28)	b8,9,10,c0	23.74	21.77	23.20	23.03	2.22	1.95	3.19	1.83
8	4(-11,-25,-26,-29)	b0,c25	18.92	20.65	20.63	21.43	1.46	1.64	1.56	1.55
9	2(-33,-34)	b0,c0	23.01	24.97	25.15	27.10	1.78	1.91	1.92	2.04
10	2(-5,-34)	b2,b10,c17	20.67	19.00	20.54	18.30	2.42	1.88	2.41	2.16
		<b>averages</b>	20.10	20.38	20.96	21.27	1.98	1.70	1.90	1.75

1. first figure is number of severe fires before the baseline period and in parentheses their timing in years before beginning of the baseline period
2. within-project period (including baseline) fires shown as events (bx or cx) during estimation periods, where b=baseline, c=crediting period and x=years after baseline or crediting period begins, and 0 indicates no severe fires during the period.

Present savanna burning methods and their associated assessment methods have been built around short term effects, like immediate emissions of combustion products and annual cycles of finer fuel accumulations and loss. They were not originally designed to deal with deep and enduring changes in temporal and spatial patterns of biomass sequestration in live and dead wood as entrained by severe fire. Clearly new approaches to assessment and carbon crediting will be required to deal with the challenges this creates for recognising and rewarding the benefits from better management to reduce frequency and scale of more severe fire events.

To summarise, while reductions in severe fire frequency can contribute to durable increases in standing AGB in lower rainfall savannas, the particular features of severe fire impacts, namely acute losses of live AGB, long recovery periods and erratic timing make local sequestration benefits hard to quantify over time scales relevant to individual fire management projects as presently conceived. Even when projects contribute to marked reductions in severe fire risk to produce collective benefits (Table S10), a substantial proportion may appear to have failed or performed weakly over time periods typically applied to assessments.